A New Model of Jupiter's Magnetic Field from Juno's First Nine Orbits

Connerney, J. E. P.; Kotsiaros, S.; Oliversen, R. J.; Espley, J. R.; Jørgensen, John Leif; Joergensen, P. S.; Merayo, José M.G.; Herceg, Matija; Bloxham, J.; Moore, K. M.

Total number of authors:
12

Published in:
Geophysical Research Letters

Link to article, DOI:
10.1002/2018GL077312

Publication date:
2018

Document Version
Publisher's PDF, also known as Version of record

AGU PUBLICATIONS

Geophysical Research Letters

RESEARCH LETTER
10.1002/2018GL077312

Key Points:
- The Juno spacecraft sampled Jupiter's magnetic field along eight polar passes separated by 45 degrees longitude affording coarse global coverage
- A degree 10 spherical harmonic model of the planetary magnetic field is obtained by partial solution of a degree 20 linear system
- Jupiter's magnetic field exhibits extraordinary hemispheric asymmetry and small-scale anomalies at the equator and at high north latitudes

Supporting Information:
- Supporting Information S1 (Text S1, Figures S1 to S6)
- Figures S7 to S22
- Figures S23 to S38
- Figures S39 to S54
- Table S1
- Table S2
- Table S3

Correspondence to:
J. E. P. Connerney,
jack.connerney@nasa.gov

Citation:
Connerney, J. E. P., Kotsiaros, S., Oliversen, R. J., Espley, J. R., Joergensen, J. L., Joergensen, P. S., et al. (2018). A new model of Jupiter's magnetic field from Juno's first nine orbits. *Geophysical Research Letters*, *45*, 2590–2596. https://doi.org/10.1002/2018GL077312

Received 26 JAN 2018
Accepted 2 MAR 2018
Accepted article online 9 MAR 2018
Published online 30 MAR 2018

A New Model of Jupiter's Magnetic Field From Juno's First Nine Orbits

J. E. P. Connerney[1,2], S. Kotsiaros[1,3], R. J. Oliversen[1], J. R. Espley[1], J. L. Joergensen[4], P. S. Joergensen[4], J. M. G. Merayo[4], M. Herceg[4], J. Bloxham[5], K. M. Moore[5], S. J. Bolton[6], and S. M. Levin[7]

[1]NASA Goddard Space Flight Center, Greenbelt, MD, USA, [2]Space Research Corporation, Annapolis, MD, USA, [3]University of Maryland, College Park, MD, USA, [4]Technical University of Denmark (DTU), Kongens Lyngby, Denmark, [5]Harvard University, Cambridge, MA, USA, [6]Southwest Research Institute, San Antonio, TX, USA, [7]Jet Propulsion Laboratory, Pasadena, CA, USA

Abstract A spherical harmonic model of the magnetic field of Jupiter is obtained from vector magnetic field observations acquired by the Juno spacecraft during its first nine polar orbits about the planet. Observations acquired during eight of these orbits provide the first truly global coverage of Jupiter's magnetic field with a coarse longitudinal separation of ~45° between perijoves. The magnetic field is represented with a degree 20 spherical harmonic model for the planetary ("internal") field, combined with a simple model of the magnetodisc for the field ("external") due to distributed magnetospheric currents. Partial solution of the underdetermined inverse problem using generalized inverse techniques yields a model ("Juno Reference Model through Perijove 9") of the planetary magnetic field with spherical harmonic coefficients well determined through degree and order 10, providing the first detailed view of a planetary dynamo beyond Earth.

Plain Language Summary Characterizing the planetary magnetic field of Jupiter is one of the primary science objectives of the Juno Mission. The Juno spacecraft was launched on 5 August 2011 and was inserted into polar orbit about Jupiter on 4 July 2016. While only one fourth of the way through its baseline mission of 34 orbits, designed to characterize the planetary magnetic field with resolution exceeding what is possible at Earth, a detailed representation of the field has emerged. The Jovian magnetic field is unlike anything previously imagined, evidencing a complexity that portends great insight into dynamo processes in general and the dynamics of Jupiter's interior in particular.

1. Introduction

Juno's primary scientific goal is to understand the origin and evolution of Jupiter, a step toward understanding the formation of our solar system and planetary systems emergent about other stars (Bolton & Juno Science Team, 2010; Bolton, Lunine, et al., 2017). The Juno mission was designed, in part, to map Jupiter's gravity and magnetic fields with extraordinary accuracy via a series of close polar passages equally spaced in longitude about the planet, eventually approximating dense global coverage. The Juno spacecraft was inserted into polar orbit about Jupiter on 4 July 2016, with perijove of ~1.05 R_j (Jupiter radius, 1 R_j = 71,492 km) and apojove of ~113 R_j. The Juno spacecraft completes an orbit in about 53 days, and the mission plan is designed to target specific perijove longitudes via slight adjustments to the orbit period. The plan provides longitudinal coverage with increasing spatial resolution, with perijoves initially separated by 90° after 4 orbits, 45° after 8 orbits, 22.5° after 16 orbits, and 11.25° after completion of the baseline mission (33 orbits, with 1 spare). Loss of data from the second perijove (PJ2) due to a spacecraft safe mode entry resulted in eight successful passes after the ninth perijove on 24 October 2017, completing coarse global sampling of the field with 45° longitudinal separation.

Prior in situ observations of Jupiter's magnetic field were limited to flyby trajectories, often quite distant from the planet, and often confined to the Jovigraphic equator, affording only limited knowledge of Jupiter's planetary field (Connerney, 2015, and references therein). Sparse data sets inescapably lead to questions regarding model uniqueness (Connerney, 1981), and the presence of distributed magnetospheric currents requires a consideration of internal/external field separation (Connerney et al., 1982). Nevertheless, observations obtained prior to the Juno mission provided spherical harmonic models of the magnetic field with model parameters through degree and order 3 reasonably well determined, particularly after

inclusion of a constraint on field geometry provided by observations of the Io Flux Tube (IFT) footprint (Connerney et al., 1998). Juno Project planning uses the degree 4 "VIP4" model (Connerney et al., 1998), based on in situ Voyager 1 and Pioneer 11 observations of the magnetic field, and a constraint provided by remote observations of the IFT footprint. This model includes degree 4 parameters that are not well resolved but needed to better fit the IFT footprint; models with terms to fifth degree (Hess et al., 2011) and seventh degree (Ridley & Holme, 2016) have also been proposed but lack model parameter resolution beyond degree 3 terms.

The very first of Juno's close passages over the surface of Jupiter was sufficient to demonstrate the complexity of the field (Bolton, Adriani, et al., 2017; Connerney, Adriani, et al., 2017) and the inadequacy of existing models. The field magnitude (7.766 Gauss) at closest approach was ~50% larger than predicted and rich with small spatial-scale variations. This is perhaps not surprising, since Juno approaches so close to the planet, particularly near perijove at a few degrees northern latitude, where no prior observation or constraint on the field exists. We note that near perijove, the spacecraft is much closer to the presumed dynamo source region (e.g., at ~0.85 R_j) than it is to neighboring periapsis passes (after nine orbits); the field is undersampled in longitude. In this paper we describe the first magnetic field model derived from Juno magnetic field observations; it is an interim model, provided in advance of the dense longitudinal coverage available later in the mission. It represents, however, a vast improvement in knowledge of Jupiter's magnetic field.

2. Methods

The magnetic field observed in Jupiter's inner magnetosphere can be regarded as the sum of contributions from several sources, led by the field due to dynamo action (interior source) inside Jupiter. At greater radial distances the magnetic field produced by distributed magnetospheric currents (exterior sources) becomes appreciable. Following earlier work (Connerney et al., 1982), we represent the magnetic field as the sum of two parts, a planetary field derivable from the gradient of a scalar potential function, V_p, and a perturbation field, **b**, due to distributed magnetospheric currents

$$\mathbf{B} = -\nabla V_p + \mathbf{b}$$

The potential V is a series expansion of spherical harmonic functions that are solutions to Laplace's equation in spherical coordinates (e.g., Chapman & Bartels, 1940):

$$V_p = a\sum_{n=1}^{n_{\max}}\left(\frac{a}{r}\right)^{n+1}\sum_{m=0}^{n}\left\{P_n^m(\cos\theta)\left[g_n^m\cos(m\phi)+h_n^m\sin(m\phi)\right]\right\}$$

where a is Jupiter's equatorial radius (71,492 km), r is the radial distance to the planet's center, and the angles θ and ϕ are colatitude and longitude, respectively. The P_n^m (cos θ) are Schmidt quasi-normalized associated Legendre functions of degree n and order m, and the g_n^m and h_n^m are the Schmidt coefficients that parameterize the internal magnetic field model. These are presented in units of Gauss or nanoteslas (1 G = 10^5 nT) for a particular choice of equatorial radius (a) of the planet. We assume that the planetary magnetic field remains constant over the interval of time (August 27, 2016 through October 24, 2017) spanned by the first nine perijoves and that Jupiter's rotation period (870.5360°/d) adequately represents the rigid rotation of the deep interior.

We use an explicit model of the magnetodisc fitted to Pioneer 10 and Voyager 1 and 2 observations (Connerney et al., 1981) to represent the field due to external currents; this model is useful within about 30 R_j of the planet. These spacecraft traversed the Jovian magnetosphere near the Jovigraphic equator and were repeatedly immersed in the magnetodisc currents over a wide range of radial distance. As such they offer a better constraint on magnetodisc model parameters; in the present analysis, we require only an approximation to the field (of order 100 nT magnitude) near the origin. Juno's orbital evolution will eventually provide magnetodisc penetration closer to the planet, at which time the distribution of magnetodisc currents will be better constrained. For the present we simply use the model derived from earlier encounters. Birkeland currents encountered traversing Jupiter's polar regions, during some passages, also contribute to the external field but are unmodeled. While they contribute fields of order hundreds of nanoteslas during some polar passages, they remain a small fraction of the measured field magnitude (few 0.1%), and their signatures are so narrowly confined that they are unlikely to bias internal field parameters.

The parameters of the model field are found by partial solution to the linear system $\mathbf{y} = \mathrm{A}\,\mathbf{x}$ relating the observations **(y)** to the *M* model parameters (**x**), consisting of the Schmidt coefficients of the spherical harmonic expansion; the magnetodisc parameters are fixed. We use all three components of the magnetic field to constrain the model parameters. The matrix A is expressed, via the singular value decomposition of Lanczos (1961), as the product of three matrices

$$\mathbf{y} = U\Lambda V^{\mathrm{T}}\mathbf{x},$$

where *U* is an *N* by M matrix consisting of the M orthonormalized eigenvectors associated with the M largest eigenvalues of $\mathbf{AA}^{\mathrm{T}}$, *V* is the M by M matrix consisting of the orthonormalized eigenvectors $V_1 \ldots V_{\mathrm{M}}$, of $\mathbf{A}^{\mathbf{T}}\mathbf{A}$ as columns, and Λ is an M by M diagonal matrix whose elements are the singular values (square roots of the eigenvalues) of $\mathbf{A}^{\mathbf{T}}\mathbf{A}$:

$$\Lambda = \begin{bmatrix} \lambda_1 & 0 & \cdots & 0 \\ 0 & \lambda_2 & & \vdots \\ \vdots & & \ddots & \vdots \\ 0 & \cdots & \cdots & \lambda_M \end{bmatrix}$$

The matrix Λ is organized in decreasing magnitude of the singular values λ_{i}, with $\lambda_{\mathrm{i}} > \lambda_{\mathrm{i}+1}$; indeed, some of the λ_{i} may be zero or very small. Solutions may be constructed by summation over the eigenvectors associated with the largest singular values

$$\mathbf{x} = \sum_{i=1}^{k} \left(\frac{\beta_i}{\lambda_i}\right)\mathbf{v}_i$$

where data vectors β_i are linear combinations of the data

$$\left(U^T\mathbf{y}\right) = \boldsymbol{\beta},$$

and the eigenvectors, $\mathbf{v}_i$, are linear combinations of the original parameters (Schmidt coefficients). Eigenvectors omitted from the solution afford insight into model nonuniqueness, and a measure of the extent to which the original parameters are estimated is provided by the diagonal elements of the resolution matrix, formed by $V_{\mathrm{k}}V_{\mathrm{k}}^{\mathrm{T}}$, where the subscript k denotes the matrix obtained by setting each column in the matrix to zero for all $i >$ k. A diagonal resolution matrix element near 1 denotes a parameter that is well resolved or recovered in the partial solution; significant off diagonal elements reveal covariability with other parameters.

The maximum degree and order required of the internal field expansion depends on the complexity of the field within the volume of space sampled. Since the Juno trajectory carries the spacecraft so close to the surface (and the source region) a spherical harmonic model with terms to high degree and order is required to follow spatial variations in the data. The concept of a partial solution allows one to extract model parameters that are well constrained even though a complete solution would require more densely spaced observations. More detailed description of the models and the inversion methodology can be found in earlier publications (Connerney, 1981; Connerney et al., 1982, 1998).

3. Observations

Observations of the vector magnetic field acquired within 7 R_j of Jupiter during these initial nine orbits were used to characterize Jupiter's planetary magnetic field. Each such orbit segment spans ~360° longitude, during which the measured magnetic field ranges from ~10^3 nT to ~10^6 nT (10 G). The magnetic field is measured at 64 samples/s with a vector accuracy of ~1 part in 10^4 (Connerney, Benn, et al., 2017) by a pair of fluxgate magnetometers located at 10 and 12 m from the spacecraft's center on a magnetometer boom extending from one of Juno's three solar arrays. Accurate attitude information is provided every 0.25 s by a pair of star cameras located with each sensor (Connerney, Benn, et al., 2017).

Juno is a spinning spacecraft with a spin period of 30 s. Our inversions used 30 s averages of the magnetic field close to the planet, and less frequent sampling at greater radial distance, according to the following scheme: one sample every 30 s for $r < 2\ R_j$, one per 60 s for $2 < r < 4\ Rj$, and 1 per 120 s for $4 < r < 7\ R_j$. Each observation was divided by an estimated standard deviation of measurement, taken as the 16 bit

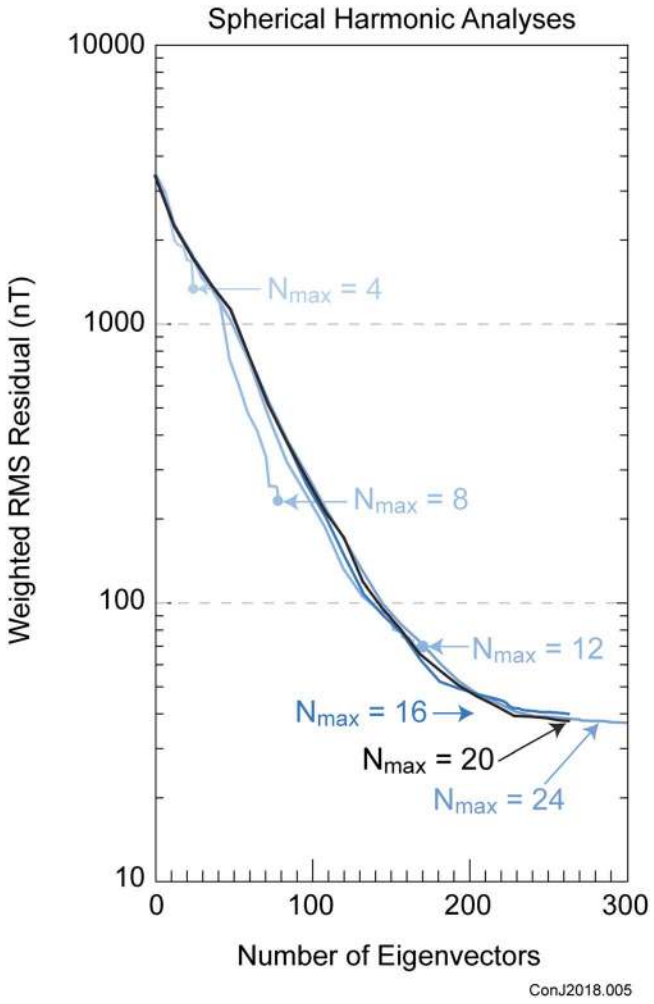

Figure 1. Goodness of fit, represented by weighted root-mean-square (RMS) residual, as a function of the number of eigenvectors included in the solution, for spherical harmonic representations of degrees 4, 8, 12, 16, 20, and 24. Each curve terminates with inclusion of all $(N_{max} + 1)^2 - 1$ eigenvectors or upon no further reduction of residuals. Increasing model complexity improves the fit to the data through degree 16–20, beyond which no significant improvement results.

quantization uncertainty ΔQ in each dynamic range, increasing by a factor of 4 with each dynamic range transition. Where ΔQ is <1 nT, 1 nT is used, reflecting a lower limit on measurement accuracy due to magnetospheric "noise." This choice was motivated by experience with prior, more distant flybys demonstrating model fits with root-mean-square residuals of a few nanoteslas (e.g., Connerney et al., 1982).

4. Results

A series of inversions with spherical harmonic models of increasing complexity (identified by the maximum degree and order of the expansion, N_{max}) provides guidance on the choice of a suitable spherical harmonic expansion, ultimately dictated by the spatial variation of the field at close-in radial distances. The family of curves in Figure 1 shows increasingly better model fits (reduced root-mean-square) obtained with increasing N_{max} through N_{max} = ~20 and no significant improvement beyond 20. Therefore, we adopt a degree and order 20 spherical harmonic to represent the planetary field and seek as complete a partial solution as afforded by the distribution of data available at present.

A model solution is constructed by summation over the independent eigenvectors of parameter space, progressing to the right in Figure 1 until minimal improvement in the fit is afforded by additional eigenvectors. The singular value decomposition, and model solution, simultaneously minimizes the misfit to the data and the magnitude of the parameter vector and therefore depends on parameter normalization. We scaled the parameter vector by r_c^{n-1} where $r_c = 0.85$ and n is harmonic degree, reflecting the expectation (and reality) of a decrease in harmonic content with increasing degree (see supporting information). A choice of $r_c = 0.85$ reflects an expectation of equal amplitudes by harmonic degree at an assumed dynamo core radius of 0.85 R_j. This scaling has the effect of increasing model parameter resolution among lower degrees relative to unweighted parameters ($r_c = 1$ R_j), a choice that would imply the expectation of equal amplitude by degree at the planet's surface.

A model constructed using 264 of the 440 possible eigenvectors is sufficient to resolve well ($R_{nn} > 0.90$; see supporting information) almost all of the spherical harmonic coefficients through degree and order 10. The subset of Schmidt coefficients through degree and order 10 is provided in the supporting information, referred hereafter as the "JRM09" model field (Juno Reference Model through Perijove 9). The model parameters are listed in machine-readable format, 1 through 120, along with the corresponding resolution matrix element and a Schmidt coefficient identifier in the supporting information. The degree 1 coefficients describe a dipole with moment M = 4.170 G, offset from the rotation axis by $\theta_d = 10.31°$ toward system 3 longitude of $\phi_d = 196.61°$.

The field magnitude computed on the surface of a dynamically flattened (1/15.4) Jupiter is illustrated with the aid of Figures 2, a rectangular latitude-longitude plot, and 3, presenting orthographic projections of the field at the poles. Each also includes the computed path of the IFT footprint compared with a recent compilation of such observations obtained from Hubble Space Telescope imagery (Bonfond et al., 2017). This comparison serves as an independent test, since these IFT observations were not used to constrain the field model in any way (unlike the VIP4 model, which included the IFT footprint locations as a constraint). A listing of the modeled satellite footprints for Amalthea, Io, Europa, and Ganymede is provided in the supporting information.

The magnetic field magnitude computed at Jupiter's surface varies from a minimum of just under 2 Gauss to a maximum of just over 20 Gauss. Surface magnetic field strengths along the IFT footprint approach a

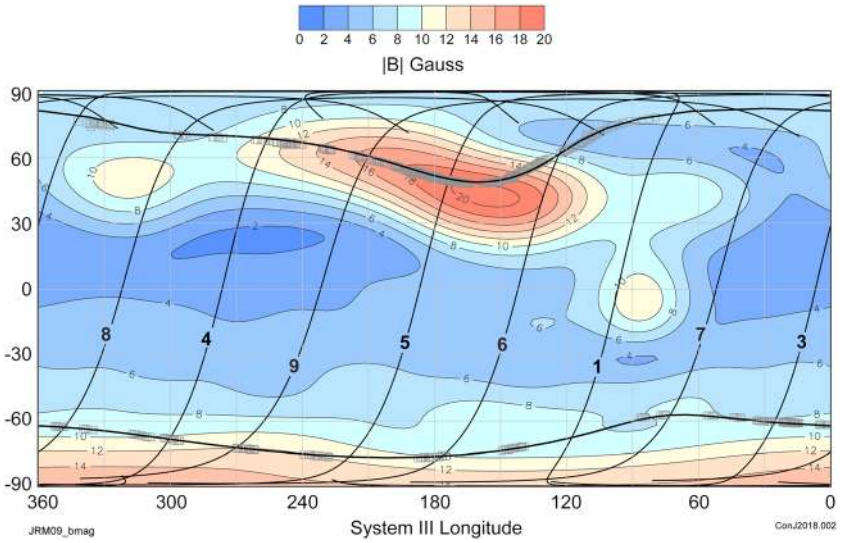

Figure 2. Contours of the magnetic field magnitude (Gauss) on the dynamically flattened (1/15.4) surface of Jupiter in rectangular latitude-longitude projection. Subspacecraft trajectory for $r < 2.5\ R_j$ is illustrated for each (numbered) perijove. Bonfond et al.'s (2017) IFT footprint observations (squares) are compared to the path of the IFT (black curve) computed from the JRM09 model.

maximum of 20 Gauss in the north (near 150° west) and 12 Gauss in the south (near 240° west), well in excess of that required to explain Io-related radio observations originating from the IFT footprint (e.g., Genova & Aubier, 1985; Hess et al., 2011). Remarkably, a map of the field magnitude using only the JRM09 terms through degree 4 appears quite similar to earlier models, which appear to have captured the field reasonably well, albeit with limited resolution.

The degree 10 representation of the field reveals an extraordinary hemispheric difference in the appearance of Jupiter's magnetic field and a peculiar isolated equatorial anomaly near 90° system 3 west longitude. This feature is the result of a reverse flux patch more clearly identified in a contour map of the radial field at 0.85 R_j presented in Figure 4. Elsewhere along the equator there appears a band of positive radial flux. Also noteworthy is a north polar anomaly evidently caused by another patch of reversed radial flux near 120°–150° west longitude. This north polar anomaly was identified previously in Hubble Space Telescope observations of the IFT footprint and aurora (Grodent et al., 2008) and implicated in connection with variable phenomena in the Jovian magnetosphere (Dessler & Hill, 1975, 1979; Hill & Dessler, 2004).

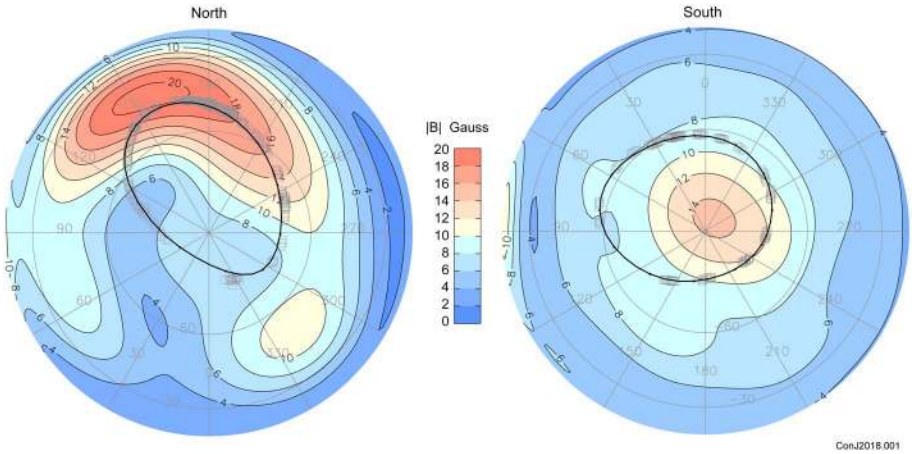

Figure 3. Same as Figure 2 but in orthographic projection.

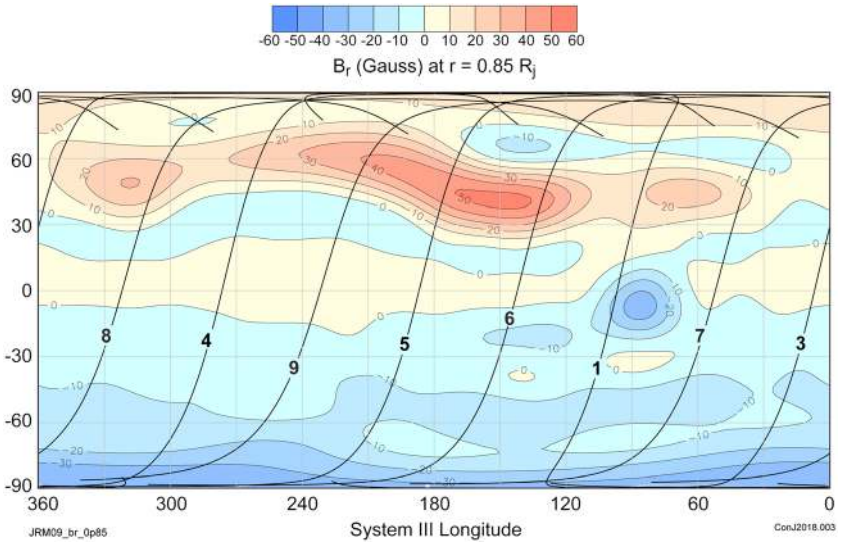

Figure 4. Contours of the radial magnetic field (Gauss) on the dynamically flattened surface with equatorial radius $r_c = 0.85\ R_j$ in rectangular latitude-longitude projection. An orthographic projection of this figure is provided in the supporting information, showing remarkable agreement with Moore et al.'s (2017) analysis (their Figure 2) of the perijove 1 observations.

Figure 5 compares the Lowes' spectrum (Lowes, 1974) computed from the JRM09 model field with that of the Earth (Langel & Estes, 1982). The Lowes spectrum offers a relative comparison of the mean square magnetic field contributed by model spherical harmonic terms of degree *n*. A magnetic field with similar amplitudes on a sphere at all spatial scales would result in a relatively flat spectrum at the corresponding radial distance, like the Earth's crustal field ($r = 1\ R_e$). The Earth's dynamo, in contrast, fits a linear trend in degree n reflecting the depth to the dynamo surface (at ~0.54 R_e). Naively interpreted, the current trend in Jupiter's Lowes' spectrum through degree 10 might imply a dynamo core surface near 0.85 R_j, although the Jovian dynamo is likely not characterized so simply as having a sharp transition between electrically conducting fluid and (relatively) insulating mantle above (like Earth's).

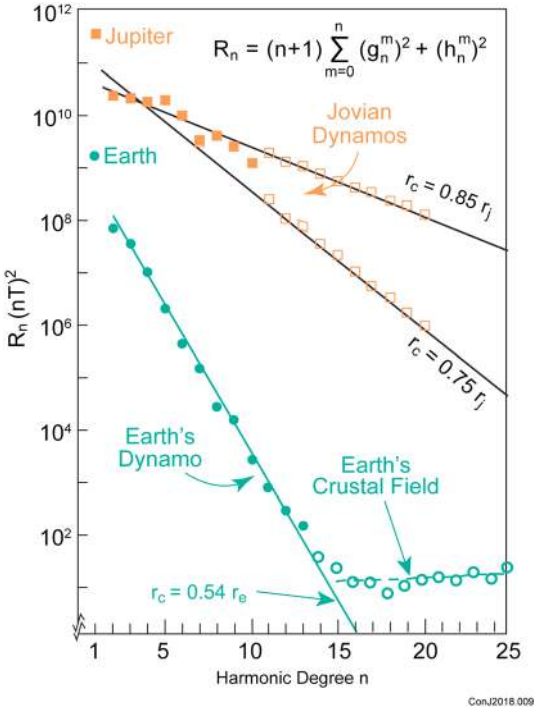

Figure 5. A comparison of the Lowes' spectrum for Earth and Jupiter using the JRM09 model magnetic field through degree/order 10.

5. Conclusions

We present a degree 10 spherical harmonic model of Jupiter's planetary magnetic field, offering the most detailed view of a planetary dynamo (other than Earth) ever obtained. This is an interim model, based on a subset of the orbital data to be acquired during Juno's baseline mission. This model will improve prediction of the field at close-in radial distances, relative to prior models, and prove useful in planning Juno's remaining orbital operations. But as yet adjacent periapsis passes are too widely spaced in longitude (~0.8 R_j at perijove) to constrain the field at the smallest spatial scales evident in observations near closest approach. Therefore, one must anticipate significant departures from the model during subsequent perijoves, as Juno slowly accumulates longitudinal coverage of the field with perijove separation (~0.2 R_j after 33 orbits) comparable to the depth to the source region.

It is premature to discuss potential secular variation of the field, although it is a topic of great interest and recent speculation (Connerney & Acuña, 1982; Ridley & Holme, 2016; Russell & Dougherty,

2010; Yu et al., 2009). While prior observations provide the advantage of a lengthy time span, these analyses are complicated by data acquisition along different and often remote flyby trajectories, and by instruments and spacecraft systems with different characteristics. The global distribution of Juno's very accurate vector observations repeated over the next several years may be expected to provide better estimates of, or limits on, Jovimagnetic secular variation.

Acknowledgments
We thank the project and support staff at the Jet Propulsion Laboratory (JPL), Lockheed Martin, and the Southwest Research Institute (SWRI) for the design, implementation, and operation of the Juno spacecraft. JPL manages the Juno mission for the principal investigator, S. Bolton, of SWRI. We especially thank Pat Lawton, Lori Spalsbury, Sidey Timmins, and Carol Ladd at GSFC for expert support. This research is supported by the Juno Project under NASA grant NNM06AAa75c to SWRI and NASA grant NNN12AA01C to JPL/Caltech. The Juno mission is part of the New Frontiers Program managed at NASA's Marshall Space Flight Center in Huntsville, Alabama. The authors are aware of no real or perceived conflicts of interest with respect to the results of this paper. As agreed with NASA, data supporting the conclusions are released on a schedule via the NASA Planetary Data System at https://pds.nasa.gov.

References

Bolton, S. J., Adriani, A., Adumitroaie, V., Anderson, J., Atreya, S., Bloxham, J., et al. (2017). Jupiter's interior and deep atmosphere: The first close polar pass with the Juno spacecraft. *Science*. https://doi.org/10.1126/science.aal2108

Bolton, S. J., & Juno Science Team (2010). The Juno mission. In *Proceedings of the International Astronomical Union Symposium* (Vol. 269, pp. 92–100).

Bolton, S. J., Lunine, J., Stevenson, D., Connerney, J. E. P., Levin, S., Owen, T. C., et al. (2017). The Juno mission. *Space Science Reviews*, *213*(1-4), 5–37. https://doi.org/10.1007/s11214-017-0429-6

Bonfond, B., Saur, J., Grodent, D., Badman, S. V., Bisikalo, D., Shematovich, V., et al. (2017). The tails of the satellite auroral footprints at Jupiter. *Journal of Geophysical Research: Space Physics*, *122*, 7985–7996. https://doi.org/10.1002/2017JA024370

Chapman, S., & Bartels, J. (1940). *Geomagnetism* (pp. 639–668). New York: Oxford University Press.

Connerney, J. E. P. (1981). The magnetic field of Jupiter: A generalized inverse approach. *Journal of Geophysical Research*, *86*, 7679–7693. https://doi.org/10.1029/JA086iA09p07679

Connerney, J. E. P. (2015). Planetary magnetism. Volume 10: Planets and satellites. In G. Schubert & T. Spohn (Eds.), *Treatise in geophysics* (Vol. 10.06, pp. 195–237). Oxford, UK: Elsevier. 978-0-444-63803-1

Connerney, J. E. P., & Acuña, M. H. (1982). Jovimagnetic secular variation. *Nature*, *297*(5864), 313–315. https://doi.org/10.1038/297313a0

Connerney, J. E. P., Acuña, M. H., & Ness, N. F. (1981). Modeling the Jovian current sheet and inner magnetosphere. *Journal of Geophysical Research*, *86*, 8370–8384. https://doi.org/10.1029/JA086iA10p08370

Connerney, J. E. P., Acuña, M. H., & Ness, N. F. (1982). Voyager 1 assessment of Jupiter's planetary magnetic field. *Journal of Geophysical Research*, *87*, 3623–3627. https://doi.org/10.1029/JA087iA05p03623

Connerney, J. E. P., Acuña, M. H., Ness, N. F., & Satoh, T. (1998). New models of Jupiter's magnetic field constrained by the Io flux tube footprint. *Journal of Geophysical Research*, *103*, 11,929–11,939. https://doi.org/10.1029/97JA03726

Connerney, J. E. P., Adriani, A., Bagenal, F., Bolton, S. J., Cowley, S., Gerard, J. C., et al. (2017). Jupiter's magnetosphere and aurorae observed by the Juno spacecraft during its first polar pass. *Science*, *356*(6340), 826–832. https://doi.org/10.1126/science.aam5928

Connerney, J. E. P., Benn, M., Bjarno, J. B., Denver, T., Espley, J., Jorgensen, J. L., et al. (2017). The Juno magnetic field investigation. *Space Science Reviews*, *213*(1-4), 39–138. https://doi.org/10.1007/s11214-017-0334-z

Dessler, A. J., & Hill, T. W. (1975). High order multipoles as a source of gross asymmetry in the distant Jovian magnetosphere. *Geophysical Research Letters*, *2*, 567–570. https://doi.org/10.1029/GL002i012p00567

Dessler, A. J., & Hill, T. W. (1979). Jovian longitudinal control of Io-related radio emissions. *The Astrophysical Journal*, *227*, 664. https://doi.org/10.1086/156777

Genova, F., & Aubier, M. G. (1985). Io-dependent sources of the Jovian decameter emission. *Astronomy and Astrophysics*, *150*, 139–150.

Grodent, D., Bonfond, B., Gerard, J.-C., Radioti, A., Gustin, J., Clarke, J. T., et al. (2008). Auroral evidence of a localized magnetic anomaly in Jupiter's northern hemisphere. *Journal of Geophysical Research*, *113*, A09201. https://doi.org/10.1029/2008JA013185

Hess, S. L. G., Bonfond, B., Zarka, P., & Grodent, T. (2011). Model of the Jovian magnetic field topology constrained by the Io auroral emissions. *Journal of Geophysical Research*, *116*, A05217. https://doi.org/10.1029/2010JA016262

Hill, T. W., & Dessler, A. J. (2004). Longitude variation of ion plasma temperature in the Io plasma torus. *Journal of Geophysical Research*, *109*, A04206. https://doi.org/10.1029/2003JA010218

Lanczos, C. (1961). *Linear differential operators* (p. 564). Princeton, NJ: D. Van Nostrand.

Langel, R. A., & Estes, R. H. (1982). A geomagnetic field spectrum. *Geophysical Research Letters*, *9*, 250–253. https://doi.org/10.1029/GL009i004p00250

Lowes, F. J. (1974). Spatial power spectrum of the main geomagnetic field and extrapolation to the core. *Geophysical Journal of the Royal Astronomical Society*, *36*(3), 717–730. https://doi.org/10.1111/j.1365-246X.1974.tb00622.x

Moore, K. M., Bloxham, J., Connerney, J. E. P., Jørgensen, J. L., & Merayo, J. M. G. (2017). The analysis of initial Juno magnetometer data using a sparse magnetic field representation. *Geophysical Research Letters*, *44*, 4687–4693. https://doi.org/10.1002/2017GL073133

Ridley, V. A., & Holme, R. (2016). Modeling the Jovian magnetic field and its secular variation using all available magnetic field observations. *Journal of Geophysical Research: Planets*, *121*, 309–337. https://doi.org/10.1002/2015JE004951

Russell, C. T., & Dougherty, M. K. (2010). Magnetic fields of the outer planets. *Space Science Reviews*, *152*(1-4), 251–269. https://doi.org/10.1007/s11214-009-9621-7

Yu, Z. J., Leinweber, H. K., & Russell, C. T. (2009). Galileo constraints on the secular variation of the Jovian magnetic field. *Journal of Geophysical Research*, *115*, E03002. https://doi.org/10.1029/2009JE003492